communications earth & environment

Article

A Nature Portfolio journal

https://doi.org/10.1038/s43247-025-02384-0

Draining of an ancient lake in the Hexi Corridor 4500 years ago triggered migration of the Hei Shan civilization

Zijuan Dong[1,2,5], Zhenbo Hu[1,2,5] ✉, Baotian Pan[1,2] ✉, David Bridgland[3] ✉, Xiaohua Li[1,2], Qinhong Mo[1,2], Menghao Li[4], Meiling Zhong[1,2] & Renzhe Pan[1,2]

Anthropolohical evidence in the Duanshankou river in the northeastern Tibetan Plateau suggests this was an important prehistoric occupation site in the Hexi Corridor, which later become part of the Silk Road, the route for trans-Eurasian trade. This study highlights the existence and potential importance of an ephemeral palaeolake, formed as a result of seismicity and environmental changes, for the prehistoric civilization in the Hexi Corridor, offering clues to the development of civilisation in this part of the Silk Road in relation to paleoenvironmental changes. Here we analyse sedimentary architecture and sequence chronology, suggesting ancient seismicity led to channel deformation in the valley floor, forming a natural dam and the resultant palaeolake. Drainage of the lake at 4.5 ka, linked to climate fluctuations, triggering human migration from the surrounding mountains to the lower reaches of the Hei River. Our findings reveal that rapid landform evolution probably influenced trans-Eurasian cultural exchange and delayed the formation of the Silk Road.

Given that early human communities would have been greatly influenced by their natural environment[1–5], the exploration of how landscape evolution has impacted the development of civilizations is of considerable value. The Silk Road has been a crucial link between East and West Eurasia, enabling trans-Eurasian cultural exchange throughout prehistory and history[6,7]. Along the Silk Road, there is much evidence (in some cases preserved as government-designated monuments) of early human activity, dating back to before the route was established[8–19] (Fig. 1a). What prevented these ancient humans from facilitating the transmission and exchange between western and eastern civilizations is an important question, pertaining not only to the historical development of the Silk Road but also to the interaction between people and the environment. Archaeological evidence indicates that the Silk Road emerged in prehistoric times, before the establishment of the Qin and Han dynasties, around 2200 BP (note that 'BP' is used in this paper to denote years before 1950 AD)[20]. The regions along the Silk Road were affected by geopolitical change, frequent wars between settlements, and changes to the natural environment, which together limited the potential for sustained interaction[21]. There has, however, been limited research specifically exploring the relationship between the evolution of civilization and environmental changes within the Silk Road region.

The Hexi Corridor in North West China, an area with an arid or semi-arid climate, is a key segment of the Silk Road and preserves, along the Hei River catchment, considerable evidence of ancient human settlements from both the prehistoric and historical periods[22], representing a great opportunity for exploring human–environment relationships. These settlements were generally short-lived[22], however, raising questions about why that was the case and whether it resulted from the influence of environmental changes in the region.

The Hei Shan rock paintings are preserved on exposed rocks on both sides of the valleys of the Duanshankou catchment, belonging to the Hei River system[23–27] (Fig. 1b, c). These rock paintings portray scenes of nomadic life (for the importance of the Hei Shan civilization within the Hei River Basin, see Supplementary Note 2), indicating that the Hei Shan region once had a rich natural environment, with forests, grasslands, rivers and abundant wildlife, including bison, large-horned deer, rhinoceros, tigers and sambar deer. These depictions suggest that the emergence of the Hei Shan civilization (as indicated by the rock paintings) dates back to ~10,000–6000 years ago, spanning the late Upper Paleolithic to Early Neolithic[24,25] (for a detailed introduction to the Hei Shan civilization, see Supplementary Note 3). The environment of that time was entirely different from that of today. The Hexi Corridor is currently extremely arid

[1]Key Laboratory of Western China's Environmental Systems (Ministry of Education), College of Earth and Environmental Sciences, Lanzhou University, Lanzhou, China. [2]Shiyang River Basin Scientific Observing Station of Gansu Province, Lanzhou, China. [3]Department of Geography, Durham University, Lower Mountjoy, South Road, Durham, UK. [4]College of Geology and Environment, Xi'an University of Science and Technology, Xi'an, China. [5]These authors contributed equally: Zijuan Dong, Zhenbo Hu. ✉e-mail: zhbhu@lzu.edu.cn; panbt@lzu.edu.cn; d.r.bridgland@durham.ac.uk

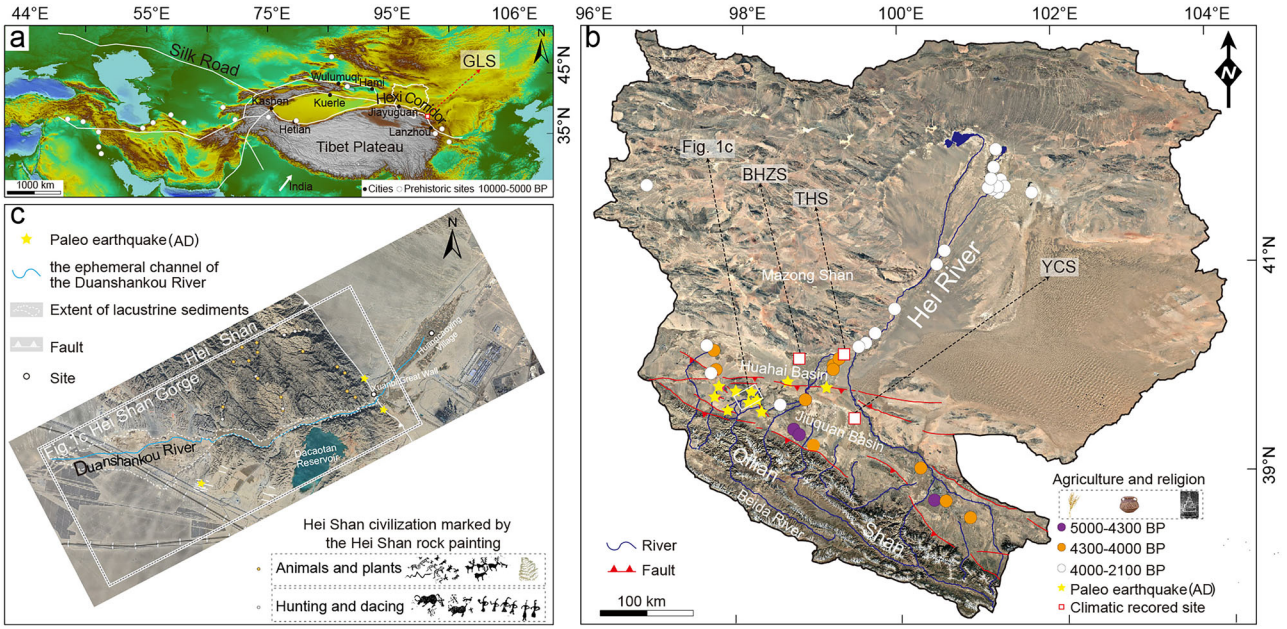

Fig. 1 | The distribution of Human civilization along the Silk Road and within the Hei River catchment. a The spatial distribution of prehistoric sites along the Silk Road within the Hei River catchment; the Hei drains northward across the Hexi Corridor. The white dotted line represents the ancient Silk Road[21]. GLS Gulang Section (climatic record). **b** Distribution of dated civilization sites dominated by agriculture and religion (purple, orange, and white dots) within the Hei River catchment. Sites from which climatic records have been obtained are also marked (white squares): BHZS Beihaizi section, THS Tiaohu section, YCS Yanchi section. **c** The spatial distribution of the Hei Shan civilization marked by the Hei Shan rock paintings within the Hei Shan Gorge, excavated by the Shuangjingzi River through the Hei Shan (Supplementary Note 4). The imagery in **b** is sourced from Google Maps ©2025 Google, with data from Landsat/Copernicus. The imagery in **c** is sourced from Google Maps (Image ©2025 Google), with data from Maxar Technologies, Airbus, and CNES/Airbus.

and completely unsuitable for hunting. Additionally, the Hei Shan petroglyphs are found only within the Duanshankou catchment, which raises the question of how the evolution of this river might have supported the development of this civilization and why the evidence is not more widespread. The term "Hei Shan Civilization" is a name we have coined in this manuscript to refer to the people responsible for the Hei Shan rock paintings. It describes the unique cultural and archeological characteristics identified in the Hei Shan region, which can be differentiated from surrounding cultures.

Of potential relevance are lacustrine sediments, preserved in the upper reach of the Duanshankou, extending over a length of 12 km within the Hei Shan Gorge (Figs. 1c and 2a). These lacustrine deposits terminate at the NNW-trending Jiayuguan Fault, which is an actively developing thrust with a dextral strike-slip. Both vertical uplift and crustal shortening rates have been estimated at ~0.1 mm/a since ~420 ka[28]. Geomorphic markers and dated landforms indicate southeastward fault propagation and hanging-wall uplift from the Hei Shan toward the modern Beida River channel[28] (Fig. 1b). Thermoluminescence dating from exploratory trenches along the Jiayuguan Fault suggests that five earthquake events occurred during the latest Pleistocene to Holocene[29]. In addition, exploratory trenches have also allowed documentation of Holocene activity of several NNW-trending subsidiary faults on the southwestern side of the main Jiayuguan Fault scarp[30,31]. Tectonic activity and climatic fluctuation are probable causes of environmental changes that notably influenced the rise and fall of the civilization represented by the Hei Shan rock paintings in this area.

As a means of exploring the evolution of the Duanshankou catchment and its links to the Hei Shan civilization, particularly in relation to climate change and tectonic activity, we focus here on the lacustrine sediments preserved on both sides of the valley. We systematically examined the sediments from seven well-exposed outcrops, looking at sedimentology, geomorphology, and chronology in the late Holocene (Meghalayan) record.

Results

Profile and chronological sequence based on optically stimulated luminescence (OSL) dating of sediments from cross-sections along the Duanshankou valley

The longitudinal profiles of rivers can provide valuable understanding of neotectonic perturbations in an area[32]. To ascertain the longitudinal profile of the Duanshankou, we surveyed the elevation of the ancient river channel employing differential GPS (Huace T12 PRO) (Fig. 2b). The valley currently occupied by the Duanshankou was originally occupied by the Shuangjingzi, a larger river that drained northwards from the Qilian Shan. Due to the coupled effects of tectonic activity and climate change, the Shuangjingzi altered its course, abandoning this section of valley, which continued to be drained by the ephemeral Duanshankou. The longitudinal profile reveals valley-floor deformation in this reach.

Furthermore, sand and silt deposits are preserved within the valley. To evaluate the sedimentary processes involved in their deposition, we conducted detailed sediment surveys at seven locations (Fig. 2), including outcrops 1 to 7 (Fig. 2b, c). A total of twelve OSL samples were taken from the seven outcrops (Fig. 2c and Table 1).

Outcrop 1, located furthest upstream, showed five main strata and a total thickness of 3.4 m. The lower unit (0.5 m). It is composed of pebble–cobble gravels. From 2.6 to 2.9 m depth, there is a 0.15-m-thick medium sand, showing distinct horizontal stratification. Mixed deposits of fine to medium gravel and cobbles from 1.8 to 2.6 m are rounded and poorly sorted. From 0.6 to 1.8 m depth, a 0.8-m-thick layer of gray–black fine and very fine sand, and gray–brown coarse to medium–coarse silt displays rhythmic alternations. This is overlain by a 0.4-m-thick gray–brown, coarse to medium–coarse silt with rhythmic alternations. The upper unit is a 0.6-m-thick layer of gravel-bearing fine sand, exhibiting visible parallel stratification. Sample O1B, from the top of the basal unit, yielded an OSL age of 9.61 ± 1.22 ka, whereas Sample OIT, from the top of the upper unit, gave 4.58 ± 0.93 ka.

A ~3.1-m-thick sedimentary sequence is exposed at outcrop 2, comprising three lithological units: the lower unit comprises 0.7 m of mixed fine

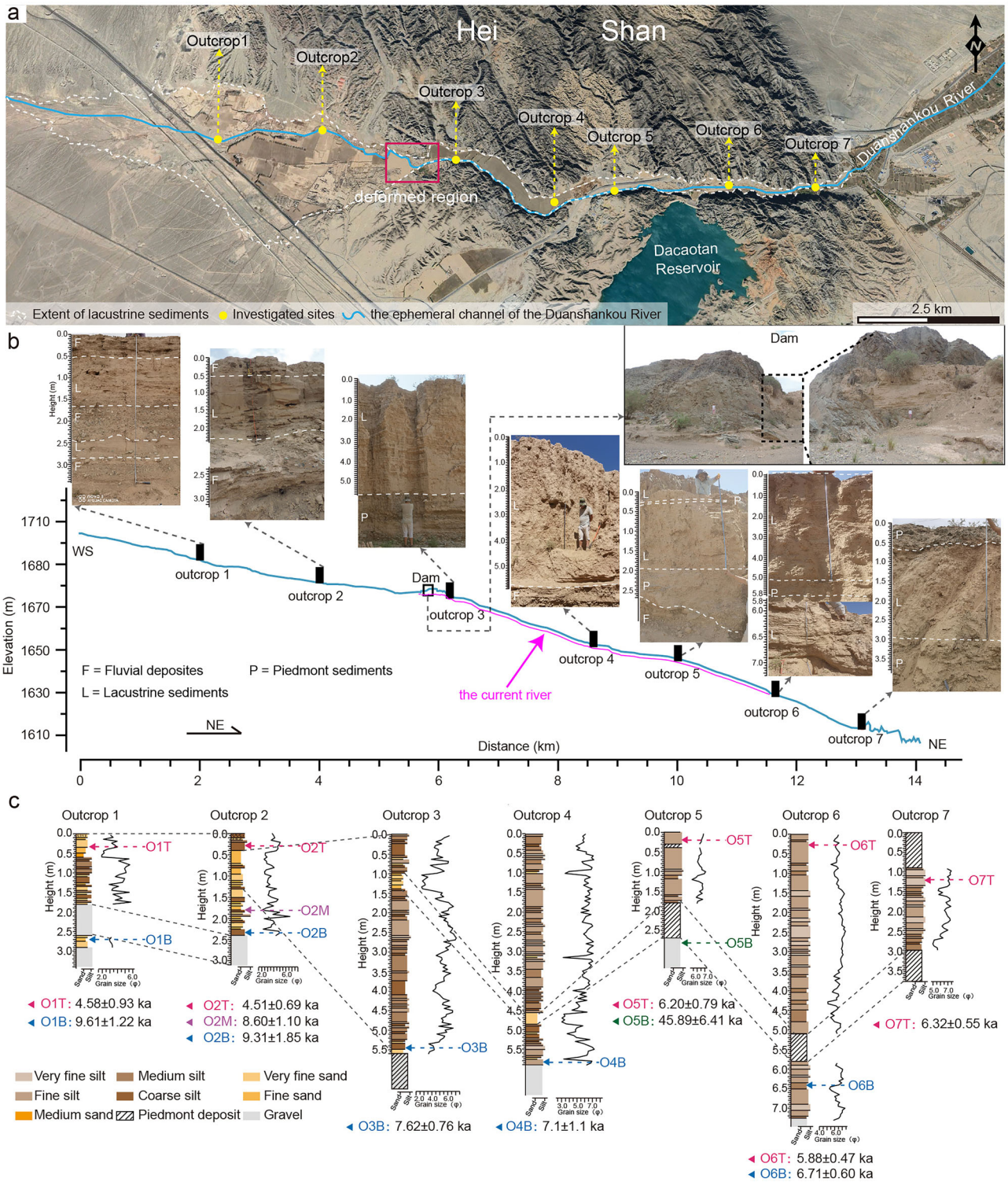

Fig. 2 | The distribution, lithological units, and chronology of lacustrine sediments, along with the longitudinal profile of the valley. a Lake deposits overlaid onto Google imagery, showing the spatial distribution of the outcrops. **b** Elevation of the ancient channel and field photos of the outcrops. We can observe from the reach between outcrops 2 and 3 that the underlying bedrock has been uplifted above the general level of the ephemeral channel of the Duanshankou. To determine the longitudinal profile of the palaeochannel, we surveyed the elevation of the modern river valley, using differential GPS (Huace T12 PRO), with an average point spacing of 0.2 m (Fig. 2b). In addition, we performed single-point measurements at locations where lacustrine deposits interface with the underlying strata (gravel layers or bedrock) exposed within the valley. These data were used to correct the modern riverbed elevation and accurately restore the palaeochannel morphology. All data were processed and visualized using ArcGIS software. The longitudinal profile of the palaeochannel reveals channel deformation affecting the river. **c** Stratigraphic panel showing lithostratigraphy, sedimentology, and OSL ages at outcrops along the modern Duanshankou River. The imagery in **a** is sourced from Google Maps (Image ©2025 Google), with data from Maxar Technologies, Airbus, and CNES/Airbus.

Table 1 | OSL sample information and analysis data

Sample number	Latitude (°N)	Longitude (°E)	Altitude (m)	OD[a] (%)	U (ppm)	Th (ppm)	K (ppm)	De (Gy)	Dose rate (mGy/a)	Age (ka)
O1T	39.82	98.06	1705	34 ± 8	1.90 ± 0.10	8.38 ± 0.42	1.57 ± 0.08	11.1 ± 2.1	2.42 ± 0.17	4.58 ± 0.93
O1B	39.82	98.06	1702	31 ± 6	2.12 ± 0.11	9.72 ± 0.49	1.65 ± 0.08	24.3 ± 2.6	2.53 ± 0.18	9.61 ± 1.22
O2T	39.83	98.07	1702	42 ± 9	1.71 ± 0.09	6.78 ± 0.34	1.51 ± 0.08	10.1 ± 1.4	2.24 ± 0.16	4.51 ± 0.69
O2B	39.83	98.07	1701	39 ± 8	1.51 ± 0.08	6.19 ± 0.31	1.09 ± 0.05	16.8 ± 3.2	1.81 ± 0.12	9.31 ± 1.85
O2M	39.82	98.08	1710	28 ± 6	1.94 ± 0.30	9.70 ± 0.60	1.66 ± 0.04	22.2 ± 2.5	2.58 ± 0.18	8.60 ± 1.10
O3B	39.83	98.10	1686	24 ± 4	2.23 ± 0.11	10.08 ± 0.50	1.47 ± 0.07	18.0 ± 1.3	2.36 ± 0.17	7.62 ± 0.76
O4B	39.83	98.12	1665	26 ± 8	0.99 ± 0.20	3.38 ± 0.40	0.90 ± 0.04	8.8 ± 1.2	1.24 ± 0.09	7.10 ± 1.10
O5T	39.84	98.13	1661	28 ± 5	2.70 ± 0.14	11.94 ± 0.60	1.90 ± 0.10	21.9 ± 2.3	3.53 ± 0.26	6.20 ± 0.79
O5B	39.84	98.13	1657	27 ± 9	2.41 ± 0.12	11.93 ± 0.60	1.73 ± 0.09	126.2 ± 15.2	2.75 ± 0.19	45.89 ± 6.41
O6T	39.84	98.15	1651	9 ± 2	2.66 ± 0.13	11.92 ± 0.60	1.93 ± 0.10	20.2 ± 0.5	3.43 ± 0.26	5.88 ± 0.47
O6B	39.84	98.15	1646	26 ± 5	2.29 ± 0.11	10.47 ± 0.52	1.72 ± 0.09	18.3 ± 1.1	2.73 ± 0.19	6.71 ± 0.60
O7T	39.85	98.17	1634	16 ± 3	2.59 ± 0.13	10.74 ± 0.54	1.92 ± 0.10	21.7 ± 1.0	3.43 ± 0.25	6.32 ± 0.55

[a]The full term for OD is overdispersion. A relatively low OD value indicates that the sample has been sufficiently bleached. We have provided the growth and bleaching curves for samples O6T and O7T in the Supplementary Materials (see Supplementary Fig. 1) to illustrate the accuracy and precision of our dating results (see Supplementary Note 1).

and medium gravels, generally poorly to modestly well rounded, with poor sorting. The middle unit is coarse silt interbedded with fine sand and showing worm burrows (Fig. 3). The upper unit consists mainly of coarse silt, with gravel. Three samples (O2B, O2M, and O2T) constrain the ages of lower, middle, and upper units, yielding ages of 9.31 ± 1.85 ka, 8.60 ± 1.10 ka, and 4.51 ± 0.69 ka, respectively.

Outcrop 3, a 5.6-m-high cliff, exposes two lithological units, a lower unit composed of coarse gravelly deposits derived from the local bedrock and an upper unit of silt. The latter is dominated by thick layers of greyish yellow–brown medium–coarse to fine silt, interbedded with multiple layers of thin gray and yellowish gray fine to very fine silt. The silt layers exhibit well-developed horizontal bedding and rhythmic layering. At a depth of 1 m below the top, there is a 0.5-m-thick layer of fine to very fine horizontally bedded sand. An OSL age of 7.62 ± 0.76 ka (sample O3B) has been determined for the base of the sequence.

Outcrop 4, with a thickness of ~6.0 m, features a basal layer of well-rounded gravel, above which are layers of greyish yellow–brown fine silt, occasionally interbedded with thin layers of yellowish gray very fine silt. The silt layers exhibit a blocky bedding structure. Sample O4B, 5.9 m from the top, yielded an age of 7.10 ± 1.10 ka.

Outcrop 5 reveals five divisions. A 2.5-m-thick layer of silts sits above well-rounded gravel and is succeeded by a 1-m-thick coarse gravelly deposit derived from the phyllite bedrock. Above this, a greyish yellow-brown fine silt layer is interbedded with thin strata of greyish yellow medium silt, showing blocky bedding features. Coarse bedrock-derived deposits are preserved at depths of 0.3–0.4 m. Chronological analysis of samples collected from the well-rounded gravel unit and the uppermost silt deposits yielded ages of 45.89 ± 6.41 ka and 6.20 ± 0.79 ka, respectively (samples O5B and O5T).

Outcrop 6 (~7.2 m thickness) is dominated by thick layers of greyish yellow–brown fine to very fine silt, intercalated with thin layers of greyish yellow medium–fine silt. The silt layers exhibit blocky bedding. From 5.1 to 5.8 m depth, there are coarse bedrock-derived deposits. Additionally, the silt layers display horizontal and rhythmic bedding. We obtained ages of 6.71 ± 0.60 ka and 5.88 ± 0.47 ka (samples O6B and O6T) from the base and top, respectively, of the sequence.

Outcrop 7, located 3.8 m above the left bank of the Duanshankou River, revealed three divisions. The bottom and top consist of 0.8 m of coarse bedrock-derived deposits. The middle division predominantly comprises thick layers of greyish yellow–brown fine to very fine silt, interbedded with thin layers of yellowish gray medium–fine silt. The silt layers exhibit massive bedding. The sediments at the top of outcrop 7 are dated to 6.32 ± 0.55 ka (sample O7T).

Discussion

In the various outcrops, we have identified fluvial, lacustrine, and colluvial (piedmont) facies. Fluvial facies appear both below and above the lake sediments. The basal gravel is well sorted and has moderate roundness, and its compositional characteristics and sedimentary structures indicate a high-energy fluvial depositional environment, suggestive of a large river draining from the northern Qilian Mountains. We attribute these deposits to the Shuangjingzi, which once occupied the Duanshankou valley (Supplementary Note 4). The laminated sands and silts, exhibiting clear lacustrine affinity, provide the record of the palaeolake, including features such as burrows.

Above the lacustrine facies are further sediments attributable to fluvial deposition, albeit differing from the basal gravels in grain size, which we interpret as representing Duanshankou drainage, following the demise of the lake. The final facies consists of layers and "stringers" of bedrock-derived detrital material that has accumulated at the edge of the valley, potentially coeval with the lacustrine silts in the valley centre.

In general, the variation in grain size directly reflects the lacustrine laminae in the seven outcrops and is closely consistent with the field observations (Fig. 2b, c). The sediments in these outcrops can be correlated based on the chronological sequence and grain size (Fig. 2c). Samples (O1B and O2B), from the bottom of lacustrine sediments in outcrops 1 and 2, yielded ages of 9.61 ± 1.22 and 9.31 ± 1.85 ka, whereas samples O1T and O2T, from the top of lacustrine sediments in the outcrops 1 and 2, were dated to 4.58 ± 0.93 and 4.51 ± 0.69 ka. Thus dates from the bottom and top of the lacustrine sediments in both outcrops are of mutually similar ages, suggesting sedimentation during the same period. This is further supported by the consistent sequence of variations in sediment grain size observed in both outcrops. The ages of samples O3B and O4B, from the bases of outcrops 3 and 4, respectively, gave ages of 7.62 ± 0.76 and 7.1 ± 1.1 ka, also indicating synchronous deposition. Sediments spanning outcrops 1–4 demonstrate coherence in grain-size distribution (Fig. 2c). Furthermore, OSL ages from samples at the bottom and top of outcrops 5–7 are predominantly 5–6 ka. Notably, within outcrop 4, a layer of very fine sands is observed at a depth of 4.5–5.0 m, potentially contemporaneous with the coarse bedrock-derived deposits in the lower parts of outcrops 5–7.

The lithostratigraphy thus consists of basal gravels, with modest rounding, attributed to fluvial transport from the Qilian Shan (Fig. 1b), followed by parallel or massive fine sand and silt, marking the formation of the lake. The uppermost fluvial gravel records the draining of the lake and reestablishment of the fluvial regime.

According to the chronological sequence and lithological correlation obtained from the outcrops, combined with the spatial distribution of

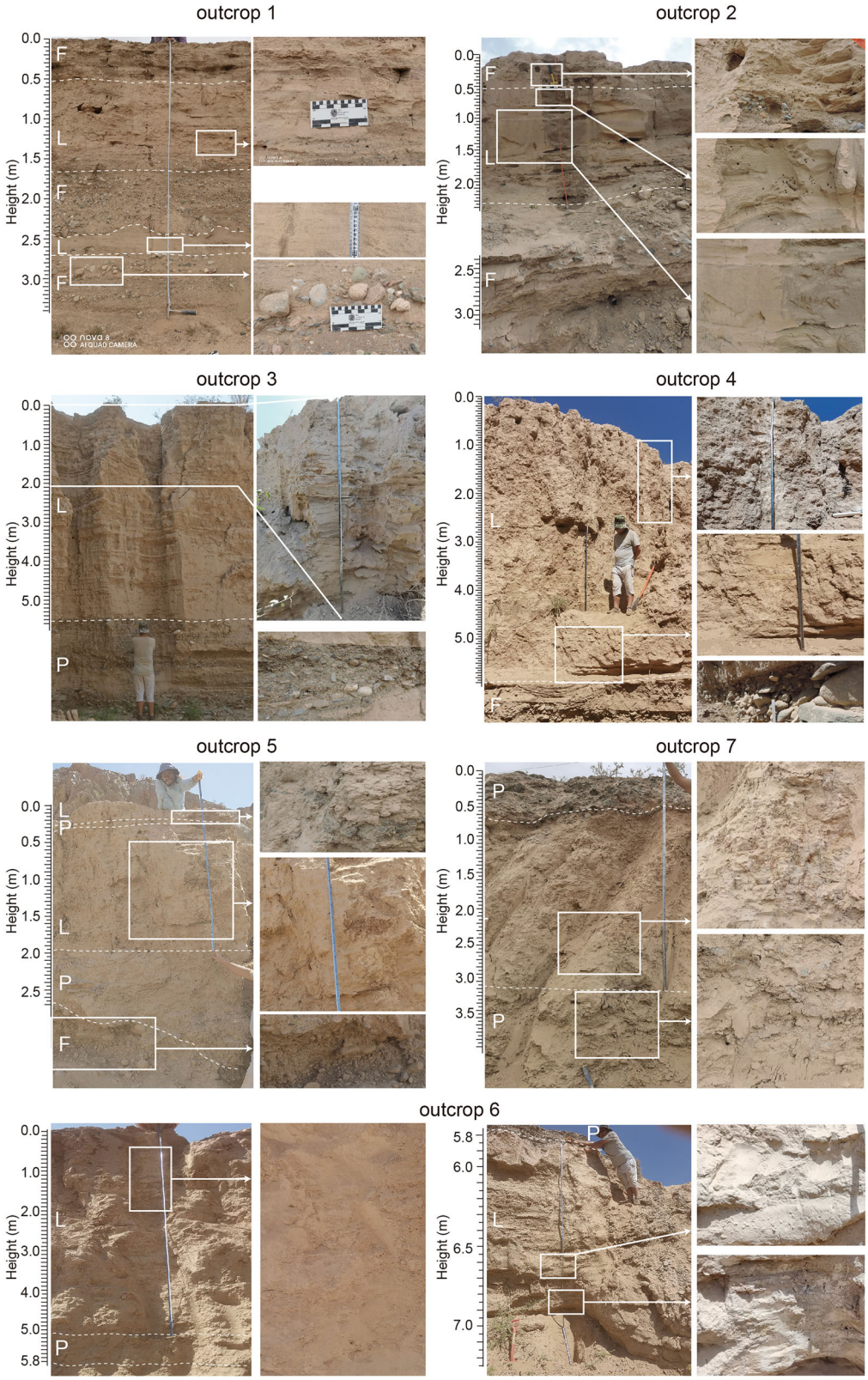

Fig. 3 | Field photos of the outcrops in the Duanshankou valley.

lacustrine sediments, it is possible to reconstruct landscape evolution in the Duanshankou valley during the Holocene (Fig. 4g). The longitudinal profile of the palaeochannel reveals deformation, indicating the formation of a natural dam that resulted in lake formation and lacustrine sedimentation.

OSL dating shows that the sediments in outcrops 1 and 2 date back to 9.5–4.5 ka, whereas those in outcrops 3–7 are concentrated between 7.6 and 6 ka. Furthermore, the longitudinal profile reveals uplifted terrain between outcrops 2 and 3 (Fig. 2b), suggesting tectonic disruption. These observations indicate that the lacustrine sediments can be divided into three

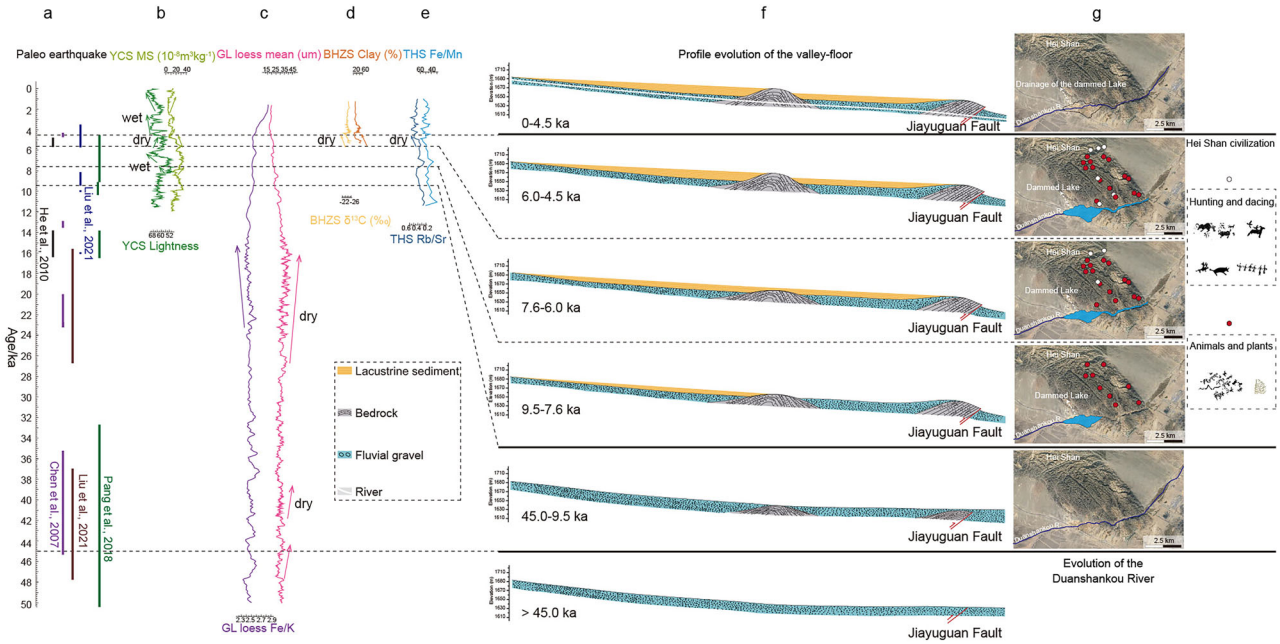

Fig. 4 | The records of climate and palaeoseismic events within the Hei River catchment, as well as the emergence and disappearance of the Hei Shan civilization with the process of landform evolution of the Duanshankou valley. **a** Palaeoseismic events of the Jiayuguan Fault and the surrounding faults[29–31,33,34]. The bars indicate chronological intervals in which palaeoseismic events occurred. **b** Climatic record from magnetic susceptibility (MS) and lightness of sediments in the Yanchi Section[42]. In China, higher/lower magnetic susceptibility (MS) is generally accepted as an indicator of ameliorated/deteriorated combinations of temperature and moisture availability in response to strengthened/weakened East Asian summer monsoon (light green). Higher/lower lightness represents lower/higher organic matter content, a reflection of drier/wetter conditions (dark green). **c** Fe/K ratio and mean grain size of GL loess[60]. A low Fe/K ratio and High mean grain size indicate a relatively dry climate. **d** Climate proxies (δ^{13}Corg and Clay) from the Beihaizi section[43]. High clay and negative δ^{13}Corg (organic carbon isotopes) values indicate a relatively humid climate in Beihaizi paleolake. **e** Climatic record from Fe/Mn and Rb/Sr ratios of sediments in the Tiaohu Section[44]. A high Rb/Sr ratio indicates weak chemical weathering intensity within the watershed, pointing to arid climatic conditions. Similarly, a high Fe/Mn ratio reflects a lowering of lake levels, suggesting a decrease in humidity in the study area. **f** Profile evolution of the valley-floor. **g** Distribution of the lacustrine sediments along the Duanshankou valley. The imagery in **g** is sourced from Google Maps (Image ©2025 Google), with data from Maxar Technologies, Airbus, and CNES/Airbus.

deposition phases. During an older phase (9.5–7.6 ka), the lake formed in the area between outcrops 1 and 2. At 7.6 ka, this region became infilled, and sedimentation expanded to the area of outcrops 3–7, lasting until ~6 ka. In a younger phase (6–4.5 ka), sedimentation continued in the area between outcrops 1 and 2, with the lake eventually disappearing at 4.5 ka (Fig. 4f, g).

Landscape evolution of this valley was indeed controlled by fault movement and climate change. The gravels beneath the lake sediments date to ~45 ka, indicating that the valley remained unblocked at that time, despite probable earlier earthquakes (Figs. 2c and 4a, f). Palaeoseismological evidence suggests that uplift resulting from fault movement could have formed a blockage (dam), obstructing upstream drainage and runoff, and thereby leading to lake formation[1]. The present research area is intersected by the Jiayuguan Fault, with five palaeo-seismic events recorded as occurring at 58.1 ka, 45.0–35.5 ka, 20.0–23.2 ka at ~12.9 ka and between 4.3 and 5.3 ka[29–31] (Fig. 4a). Furthermore, there are records of palaeoseismic events from the same periods affecting other faults in the vicinity of the Jiayuguan Fault[33,34] (Figs. 1b and 4a). Earthquakes occurring before 12.9 ka, and coupled with drying climate, likely contributed to deformation of the Duanshankou valley. At 9.5 ka, the magnitude of vertical displacement exceeded the river's incision capacity, resulting in damming and lake formation. Climatic records from the Yanchi (YCS), Gulang (GLS), Beihaizi (BHZS), and Tiaohu (THS) sections (Figs. 1a, b and 4b–e) in the Hexi Corridor indicate that the climate was warm and humid at 9.5 and 6 ka. The abundant precipitation would have promoted lake formation as well as the input of copious sediment, eventually resulting in infill and potential overflow of the lake. Seismic activity between 5.3 and 4.3 ka caused further deformation, increasing the accommodation space and facilitating continued lacustrine sedimentation until ~4.5 ka. This coincided with a period of arid climate, marked by decreased precipitation and reduced sediment supply, which ultimately caused the cessation of lake sedimentation. As the climate became progressively wetter after 4.5 ka, the Duanshankou River began to incise, eventually leading to the destruction of the lake.

Therefore, the evidence for lacustrine conditions preserved in the Duanshankou catchment may have resulted from a combination of tectonic activity and climate change. There are similar examples of lake formation from other parts of the world. For instance, a lake located within the frontal thrust belt of the Betic Cordillera, SE Spain, is dammed by an antithetic fault[1]. Similarly, this phenomenon is also observed in Mississippi drainage[2].

The processes of fluvial response to climate fluctuation and tectonic activity have played key roles in the evolution of ancient civilizations[35]. Based on the sediment chronology, the lake within the Duanshankou catchment was formed at ~9.6 ka and disappeared at ~4.5 ka. It would have provided a habitat for a wide range of wildlife and nurtured the civilization responsible for the Hei Shan rock paintings[24,25] (Fig. 4g). The rock art depicts scenes of ancient humans primarily engaged in hunting, with illustrations of them using bows and arrows (Supplementary Fig. 2). Yao et al.[19] reported the presence of arrowheads in this region dating back to 7–5 ka, further supporting linkage between the Hei Shan civilization and the evolution of the Duanshankou River. Moreover, the depiction of ferns in these rock paintings has important environmental implications, as such plants were only present in the Hexi Corridor during the warm period from 11,000 to 7000 years ago[24]. This timeframe provides an ecological basis for dating the rock paintings. Notably, the arrangement of dancers in sequences and the design of their headdresses, featuring dance motifs found in the Hei Shan rock paintings, bear similarities to those in various cultures across different periods and geographical regions[36]. These patterns bear a striking resemblance to the painted pottery designs of the Halaf and Ubaid cultures in Mesopotamia from 6000 to 7000 years ago, as well as to rock paintings,

painted pottery, and other decorative artefacts found in the Indus Valley, West Asia, Southern Europe, the Americas, and Russia[36]. This transcontinental cultural similarity, combined with the unique geographical location of the Hexi Corridor and its network of rivers flowing through mountain passes, strongly suggests that the region may have served as a crucial hub for Eurasian cultural exchanges during prehistoric times.

The challenges associated with inferring the age of rock art solely from motif content should be carefully noted, however. Specifically, motif-based analysis is constrained by factors related to cultural diffusion, individual artistic expression, and regional variation, making chronological attribution based solely on style potentially unreliable[37]. Furthermore, many motifs, such as human figures, animals, and hunting scenes, are widely used across different time periods and regions, leading to ambiguity in chronological attribution[38]. Additionally, cultural continuity or revival may result in similar symbols appearing in different periods, further complicating precise dating. The preservation state of the rock art also poses challenges, as weathering, erosion, and other natural processes over time can obscure or damage critical details necessary for stylistic comparison[39]. Most importantly, the absence of direct dating methods or associated archeological materials for the rock art itself means that chronological interpretation based on content remains speculative without independent chronological control[40].

Nonetheless, the three lines of evidence (bow and arrow technology, fern depictions, and dance motifs) mutually reinforce each other, collectively illustrating how prehistoric humans might have adapted to the natural environment of the Hexi Corridor while simultaneously developing complex social networks through technological diffusion and cultural exchange. With the lake disappearing at ~4.5 ka, abundant water resources appeared in the lower reaches of the Beida and Hei rivers (Fig. 1b), leading to migration of the civilization from the foothills of the He Shan and Qilian Shan to the downstream delta, where agriculture flourished (Fig. 1b). During this period, the upper reaches of the Beida River also stabilized[41]. The stability of the river system and abundant water resources facilitated the further development of human civilization, giving rise to the agricultural civilization of the Hexi Corridor. With their basic needs met, the humans of the delta began to explore religious culture, and their long-term settlement eventually facilitated the establishment of the Silk Road. This indicates that localized environmental changes had a profound impact on the succession of prehistoric settlements, with environmental and landscape change forcing migration of human habitation. Similar cases have been documented in Indus Civilization, human migration in the Taklimakan desert, and Loulan Civilization in the Lop Nur[3–5].

Lacustrine sediments in the area near the Duanshankou (Such as at Yanchi, Beihaizi, and Tiaohu: see Fig. 1b) have been investigated previously, with particular focus on chemical indicators and climatic reconstruction; there is a lack of data from microfossils[42–44]. Moreover, studies of lacustrine sediments from the broader region, such as those in Lake Qinghai[45,46], Lake Bosten[47], Lake Daihai[48], and Lake Donggi Cona[49,50], have also provided valuable data. This suggests that there is substantial potential for further research on the deposits of the Duanshankou palaeolake.

Conclusions

We suggest that palaeo-seismic activity coupled with climate change, by disrupting drainage in the Duanshankou valley to form a dammed lake, had a profound influence on the prehistoric civilization in this region. This lake would have offered long-lived (5 ka) favorable conditions that provisioned the Hei Shan civilization, well-known for the rock art they left. However, when the lake disappeared, the civilization was forced to migrate. Our results firmly suggest that the absence of early transmission between Eastern and Western civilizations was largely attributable to this disruptive and rapid landscape evolution, driven by tectonic activities and climate change at the northeastern margin of the Tibetan Plateau.

Methods

Sampling

As one of the main characteristics of deposits, grain size can reflect the dynamic type and transport mode of a transportation medium. In addition, granularity indices can be used as a basis for the analysis and explanation of genetic environments[51]. Analyzes of particle-size distribution have been widely used in the field of sedimentology as a key part of research on the evolution of geological environments[52] and for the reconstruction of palaeoclimate and palaeoenvironment[53].

To reconstruct the evolution of the Duanshankou valley, seven representative sections of lacustrine sediments, namely the sampling sites outcrops 1–7, were chosen for grain size analysis (Fig. 2b). A total of 454 samples were taken at 0.05-m intervals from the upper lacustrine sediments in the seven outcrops. Moreover, 12 optically stimulated luminescence (OSL) dating samples were collected from the lower and upper parts of the outcrops. The OSL samples were collected from fine sand and silt layers in lacustrine sediments. During sampling, after cutting back 30 cm of surface material, a 30 cm-long stainless-steel tube was hammered horizontally into the newly excavated vertical section. Immediately after removal, the tube, containing the sample, was sealed at both ends with tinfoil and tape.

Grain-size analysis

All samples for grain-size measurement were analyzed at the Key Laboratory of Western China's Environment Systems, Ministry of Education, China. They were boiled at 180 °C with 30% hydrogen peroxide (H_2O_2) to remove organic matter and then with 10% hydrochloric acid (HCl) to remove carbonates. Furthermore, ultrasonic pretreatment, coupled with the addition of 20% $(NaPO_3)_6$ solution, was also used to disperse the particles from each other for subsequent grain-size determination. Finally, these processed samples were measured with a Malvern Mastersizer 2000 to obtain grain-size distribution[54] (Fig. 2c).

OSL dating

Sample preparation for luminescence measurements took place at the Qinghai Institute of Salt Lakes, Chinese Academy of Sciences. From the innermost material in the sampling tubes, quartz grains (90–125 μm) were extracted using conventional sample preparation procedures (HCl, H_2O_2, sieving, density separation, and etching for 60 min with 40% HF). The purity of the quartz extracts was confirmed by the absence of a significant infrared stimulated luminescence (IRSL) response at 60 °C to a regenerative β-dose. The sensitivity to infrared stimulation was considered to be significant if the resulting IRSL signal amounted to more than 10% of the corresponding OSL signal[55] or if the OSL IR depletion ratio deviated by more than 10% from unity[56]. The luminescence measurements were made with a Risø TL/OSL-DA-20 reader, equipped with high-power blue diodes emitting at 470 ± 20 nm and IR diodes emitting at 830 nm. All luminesce32nce emissions were detected through a 7.5 mm thick Hoya U-340 UV filter. Irradiations were carried out with a $^{90}Sr/^{90}Y$ β-source mounted on the reader. The equivalent dose (De) was determined using the single-aliquot regenerative-dose (SAR) and standard growth curve (SGC) protocol as described by Murray and Wintle[57]. The environmental dose rate was calculated from the concentrations of U, Th, and K in the samples and from the contribution of cosmic rays[58]. The water content was estimated according to the natural water content and saturated water content. The annual dose can be calculated according to the formula and parameters provided by Aitken[59]. All OSL sample information and age results are presented in Table 1[54].

Reporting summary

Further information on research design is available in the Nature Portfolio Reporting Summary linked to this article.

Data availability

All data needed to evaluate the conclusions in the paper are present in the paper and the Supplementary Information. Links to data are provided below: https://doi.org/10.6084/m9.figshare.28927397.

Received: 7 December 2024; Accepted: 14 May 2025;
Published online: 23 May 2025

References

1. Rodríguez-Pascua, M. A., Pérez-López, R., Calvo, J. P. & García del Cura, M. A. Recent seismogenic fault activity in a Late Quaternary closed-lake graben basin (Albacete, SE Spain). *Geomorphology* **102**, 169–178 (2008).
2. Guccione, M. J. et al. Stream response to repeated coseismic folding, tiptonville dome, new madrid seismic zone. *Geomorphology* **43**, 313–349 (2002).
3. Singh, A. et al. Counter-intuitive influence of Himalayan River morphodynamics on Indus Civilisation urban settlements. *Nat. Commun.* **8**, 1617 (2017).
4. Li, K. et al. Hydrological change and human activity during Yuan–Ming Dynasties in the Loulan area, northwestern China. *Holocene* **28**, 1266–1275 (2018).
5. Sun, A. et al. Southward retreat of the Keriya River drove human migration in the Taklimakan Desert during the late Holocene. *Quat. Sci. Rev.* **332**, 108665 (2024).
6. Flad, R., Li, S. C. & Wu, X. H. Early wheat in China: results from new studies at Donghuishan in the Hexi Corridor. *Holocene* **20**, 955–965 (2010).
7. Yang, Y. et al. Economic change in the prehistoric Hexi Corridor (4800–2200 BP), North-West China. *Archaeometry* **61**, 957–976 (2019).
8. Willcox, G. Carbonized plant remains from Shortughai, Afghanistan. In: Renfrew J. M., ed. *New Light on Early Farming: Recent Developments in Palaeoethnobotany* (Edinburgh University Press, 1991).
9. Harris, D. R. et al. Investigating early agriculture in Central Asia: new research at Jeitun, Turkmenistan. *Antiquity* **67**, 324–338 (1993).
10. Su, L. *On the Culture of Stone Age in Central Asia*. Master's thesis, Guizhou Normal Univ. (2005).
11. Isakov, A., Kohl, P. L., Lamberg-karlovsky, C. C. & Maddin, R. Metallurgical analysis from Sarazm, Tadjikistan SSR. *Archaeometry* **29**, 90–102 (2007).
12. Frachetti, M. D., Spengler, R. N., Fritz, G. J. & Mar'yashev, A. N. Earliest direct evidence for broomcorn millet and wheat in the central Eurasian steppe region. *Antiquity* **84**, 993–1010 (2010).
13. Doumani, P. N. et al. Burial ritual, agriculture, and craft production among Bronze Age pastoralists at Tasbas (Kazakhstan). *Archaeol. Res. Asia* **1-2**, 17–32 (2015).
14. Shi, Z. *Research on Environmental Change of Hei River Basin in Historical Period.* Lanzhou Univ. (2017).
15. Jiang, J. The Cuneiform civilization from the perspective of dialogue between civilizations. *His. Teach.* **8**, 65–72 (2019).
16. An, C. et al. The Holocene environmental change in Xinjiang and its impact on prehistoric cultural exchange. *Sci. Sin. Terrae* **50**, 677–687 (2020).
17. Wang, H. On the origin of civilization in mesopotamia of ancient West Asia. *J. Tangshan Norm. Univ.* **44**, 97–101 (2022).
18. Zhu, X. *Comparative study of bronze plastic arts in Sanxingdui and West Asia. Sichuan Conservatory of Music*. Master's thesis (2023).
19. Yao, J. et al. The evolution of prehistoric arrowheads in northern China and its influential factors. *Sci. China Earth Sci.* **66**, 2109–2124 (2023).
20. Dong, G., Yang, Y., Han, J., Wang, H. & Chen, F. Exploring the history of cultural exchange in prehistoric Eurasia from the perspectives of crop diffusion and consumption. *Sci. China Earth Sci.* **60**, 1110–1123 (2017).
21. Cao, H., Wang, Y., Qiu, M., Shi, Z. & Dong, G. On the Exploration of Social Development during a Historical Period in the Eastern Tienshan Mountains via Archaeological and Geopolitical Perspectives. *Land* **11**, 1416 (2022).
22. Yang, Y. et al. Copper content in anthropogenic sediments as a tracer for detecting smelting activities and its impact on environment during prehistoric period in Hexi Corridor, Northwest China. *The Holocene* 1–10. https://doi.org/10.1177/0959683616658531 (2016).
23. Chu, S., Han, J. & Li, Y. Ancient rock paintings in black mountain, Jiayuguan, Gansu. *Archaeology* **04**, 344-359+389-392 (1990).
24. Hu, X. Survey on the conservation and utilization of the Hei Shan rock Paintings in Jiayuguan. *Silk Road* **000**, 71–74 (2012).
25. Gao, Y. Protecting and utilizing the Hei Shan rock paintings to promote the cultural industry development of Jiayuguan City. *Cult. Heritage* **12**, 2 (2016).
26. Guo, X., Sun, Y. & Zhang, B. An observation and study of Petroglyph in Gansu Province. *Gansu Rock Art Investig.* **15**, 23–36 (2018).
27. Feng, G. *Visual design based on the Hei Shan rock painting in Jiayuguan* (Lanzhou University, 2020).
28. Yang, H. et al. Diachronous Quaternary development of the Jiayuguan Fault and implications for strain compartmentalization and modern earthquake hazards in the NW Hexi Corridor, China. *Tectonics* **42**, e2023TC007753 (2023).
29. Chen, B., Liu, J., Zhang, Y. & Liu, J. Late Quaternary neotectonic movement of the Jiayuguan fault. *J. Geomech.* **13**, 78–85 (2007).
30. He, W., Yuan, D., Wang, A., Liang, M. & Zheng, W. The recent active characteristics of the Middle Segment of Jiayuguan Fault. *Earthq. Res. China* **26**, 296–303 (2010).
31. Liu, X., Wu, Z., Liang, M., Yuan, D. & He, W. Paleoearthquake characteristics of the Jiayuguan fault and its seismic risk. *Earth Sci.* **46**, 3796–3806 (2021).
32. Phartiyal, B., Singh, R. & Kothyari, G. C. Late-Quaternary geomorphic scenario due to changing depositional regimes in the Tangtse Valley, Trans-Himalaya, NW India. *Palaeogeogr. Palaeoclimatol. Palaeoecol.* **422**, 11–24 (2015).
33. Liu, X., Yuan, D., He, W., Shao, Y. & Zhang, B.Research progress on paleoearthquakes in Jiuxi Basin, located in the western Hexi Corridor. *China Earthquake Eng. J.* **43**, 1–10 (2021).
34. Pang, W., Zhang, B., He, W. & Wu, M. Preliminary study of paleoearthquakes on the middle-eastern segment of Jintanan Shan Fault. *Seismol. Geol.* **40**, 801–817 (2018).
35. Fan, S. et al. Debris flow events of 4000 a BP and its resulting archaeological site destruction in Qian River gorge, the upper reach of Wei River, central China. *Geol. J.* **55**. https://doi.org/10.1002/gj.3879 (2020).
36. Zhang, Q. A preliminary study on the ethnic identity of the early creators of Hei Mountain petroglyphs—an interpretation of the queue dance petroglyphs. In *Proc. Silk Road Painted Pottery and Jiayuguan Historical and Cultural Symposium* (Lanzhou University Press, 2017).
37. Conkey, M. W. The identification of prehistoric hunter-gatherer aggregation sites: the case of Altamira. *Curr. Anthropol.* **21**, 609–630 (1980).
38. Bednarik, R. G. The dating of rock art: a critique. *J. Archaeol. Sci.* **29**, 1213–1233 (2002).
39. Martínez-Pabello, P. U. et al. Rock varnish as a natural canvas for rock art in La Proveedora, northwestern Sonoran Desert (Mexico): Integrating archaeological and geological evidences. *Quat. Int.* **572**, 74–87 (2021).
40. Aubert, M. et al. Pleistocene cave art from Sulawesi, Indonesia. *Nature* **514**, 223–227 (2014).
41. Pan, B. et al. Channel migration in the northeastern margin of the Tibetan Plateau and its implication for fluvial response to the interaction between rapid tectonic activity, climatic fluctuation and human influence. *Quat. Sci. Rev.* **310**, 108126 (2023).
42. Yu, Y. et al. Millennial-scale Holocene climate variability in the NW China drylands and links to the tropical Pacific and the North Atlantic. *Palaeogeogr. Palaeoclimatol. Palaeoecol.* **233**, 149–162 (2006).
43. Peng, S. et al. Middle to Late Holocene lake evolution and its links with westerlies and Asian monsoon in the middle part of the Hexi Corridor, NW China. *Quat. Res.* **116**, 30–45 (2023).
44. Li, X., Liu, H., Zhao, K., Ji, M. & Zhou, X. Holocene climate and environmental changes reconstructed from elemental geochemistry in the western Hexi Corridor. *Acta Anthropol. Sin.* **32**, 110–120 (2013).

45. Hu, Z., Wang, X., Pan, B., Bridgland, D. & Vandenberghe, J. The quaternary of the upper Yellow River and its environs: field guide. *Quaternary Res. Assoc.* 1–84 (2017).
46. Yan, D., Wünnemann, B. & Zhang, Y. Late Quaternary lacustrine Ostracoda and their implications for hydro climatic variation in Northeastern Tibetan Plateau. *Earth Sci. Rev.* **207**, 103251 (2020).
47. Xiang, L. et al. First Pediastrum–temperature transfer function and its application to mid-to-late Holocene reconstruction in Central Asia. *Quat. Sci. Rev.* **327**, 108516 (2024).
48. Chen, L. et al. Drought in the Asian summer monsoon region is liked to a weakened interhemispheric temperature gradient. *Commun. Earth Environ.* **5**, 432 (2024).
49. Dietze, E. et al. Early to mid-Holocene lake high-stand sediments at Lake Donggi Cona, northeastern Tibetan Plateau, China. *Quat. Res.* **79**, 325–336 (2013).
50. Saini, J. et al. Climate variability in the past ~19,000 yr in NE Tibetan Plateau inferred from biomarker and stable isotope records of Lake Donggi Cona. *Quat. Sci. Rev.* **157**, 129–140 (2017).
51. Poizota, E., Mear, Y., Thomas, M. & Garnaud, S. The application of geostatistics in defining the characteristic distance for grain size trend analysis. *Comput. Geosci.* **32**, 360–370 (2006).
52. Tu, L. et al. Holocene East Asian winter monsoon changes reconstructed by sensitive grain size of sediments from Chinese coastal seas: a review. *Quat. Int.* **440**, 82–90 (2017).
53. Stanley, J. D. & Clemente, P. L. Clay distributions, grain sizes, sediment thicknesses, and compaction rates to interpret subsidence in Egypt's northern Nile Delta. *J. Coast. Res.* **30**, 88–101 (2014).
54. Dong, Z. et al. Source data for "Draining of an ancient lake in the Hexi Corridor 4500 years ago triggered migration of the Hei Shan civilization" [Dataset]. *Figshare*. https://doi.org/10.6084/m9.figshare.28927397 (2025).
55. Vandenberghe, D. *Investigation of the Optically Stimulated Luminescence Dating Method for Application to Young Geological Sediments*. Ph.D. thesis Universiteit Gent, 298 (2004).
56. Duller, G. A. T. Distinguishing quartz and feldspar in single grain luminescence measurements. *Radiat. Meas.* **37**, 161–165 (2003).
57. Murray, A. S. & Wintle, A. G. The single aliquot regenerative dose protocol: potential for improvements in reliability. *Radiat. Meas.* **37**, 377–381 (2003).
58. Prescott, J. R. & Hutton, J. T. Cosmic ray contributions to dose rates for luminescence and ESR dating: large depths and long-term time variations. *Radiat. Meas.* **23**, 497–500 (1994).
59. Aitken, M. J. Thermoluminescence dating. London: Academic Press 359. https://doi.org/10.2307/281807 (1985).
60. Sun, Y. et al. Persistent orbital influence on millennial climate variability through the Pleistocene. *Nat. Geosci.* **14**, 812–818 (2021).

Acknowledgements

This research was financially supported by the National Natural Science Foundation of China (Grant no. 41730637), the Fundamental Research Funds for the Central Universities (Grant no. lzujbky-2022-ey10), and the "Innovation Star" Project for Postgraduate Students of Gansu Province, People's Republic of China (Grant no. 2025CXZX-082). We deeply appreciate Professor Yixuan Wang for her support with the laboratory analyzes, Professor Dongju Zhang for her assistance in constraining the chronological framework of the Hei Shan rock paintings, and Professors Daoyang Yuan and Xiaofei Hu for their valuable insights into the tectonic activity discussed in the manuscript. We are also truly grateful to Shiping Wei, our driver, for his valuable assistance during fieldwork and sample collection. No specific permissions were required for the sampling conducted in this study, as all activities complied with relevant regulations and did not involve protected species or access to private land.

Author contributions

All co-authors have participated in the development of this manuscript and approved its submission to the journal. Zijuan Dong was responsible for investigation, formal analysis, data curation, and preparation of the original draft. Zhenbo Hu developed the main idea and led the project administration, conceptualization, supervision, and reviewing and editing the manuscript. Baotian Pan supervised funding acquisition and contributed to project administration and conceptual development. David Bridgland supported project administration, helped shape the conceptual framework, played a key role in reviewing and editing, and managed data curation. Qinhong Mo, Xiaohua Li, Menghao Li, Meiling Zhong, and Renzhe Pan were involved in data curation and field investigations.

Competing interests

The authors declare no competing interests.

Additional information

Supplementary information The online version contains supplementary material available at https://doi.org/10.1038/s43247-025-02384-0.

Correspondence and requests for materials should be addressed to Zhenbo Hu, Baotian Pan or David Bridgland.

Peer review information *Communications Earth & Environment* thanks Jianhui Jin and the other, anonymous, reviewer(s) for their contribution to the peer review of this work. Primary Handling Editors: Gareth Roberts and Carolina Ortiz Guerrero. A peer review file is available.